	Mayeux, Richard; Columbia University, Neurology Brickman, Adam; Columbia University, ;
Keywords:	white matter hyperintensities, Alzheimer's disease, autosomal dominant
Domain:	Clinical and/or Desktop Research

SCHOLARONE™
Manuscripts

Accepted Article

This is the author manuscript accepted for publication and has undergone full peer review but has not been through the copyediting, typesetting, pagination and proofreading process, which may lead to differences between this version and the Version record. Please cite this article as doi:10.1002/ana.24647.

This article is protected by copyright. All rights reserved.

White matter hyperintensities are a core feature of Alzheimer's disease: Evidence from the Dominantly Inherited Alzheimer Network

Running head: White matter hyperintensities in familial AD

Seonjoo Lee, PhD[3,4,¥], Fawad Viqar, MA[1,2,¥], Molly E. Zimmerman, PhD[2,5], Atul Narkhede, MS[1], Giuseppe Tosto, MD, PhD[1,6], Tammie L.S. Benzinger, MD, PhD[7], Daniel S. Marcus, PhD[7], Anne M. Fagan, PhD[8], Alison Goate, PhD[9], Nick C. Fox, MD[10], Nigel J. Cairns, PhD[11], David M. Holtzman, MD[8], Virginia Buckles, PhD[8], Bernardino Ghetti, MD[12], Eric McDade, DO[8], Ralph N. Martins, PhD[13], Andrew J. Saykin, PsyD[14], Colin L. Masters, MD[15], John M. Ringman, MD[16], Natalie S. Ryan, MBBS[10], Stefan Förster, MD[17], Christoph Laske, MD[18], Peter R. Schofield, PhD, DSc[19], Reisa A. Sperling, MD[20], Stephen Salloway, MD[21], Stephen Correia, PhD[22], Clifford Jack Jr, MD[23], Michael Weiner, MD[24], Randall J. Bateman, MD[8], John C. Morris, MD[8], Richard Mayeux, MD[1,6,25], and Adam M. Brickman, PhD[1,6,25]*
for the Dominantly Inherited Alzheimer Network

1. Taub Institute for Research on Alzheimer's Disease and the Aging Brain, College of Physicians and Surgeons, Columbia University, New York, NY USA
2. Psychology Department, Fordham University, Bronx, NY USA
3. Department of Psychiatry, College of Physicians and Surgeons, Columbia University, New York, NY USA
4. Department of Biostatistics, Mailman School of Public Health, Columbia University, New York, NY USA
5. Department of Neurology, Albert Einstein College of Medicine, Bronx, NY USA
6. Department of Neurology, Columbia University Medical Center and the New York Presbyterian Hospital, Columbia University, New York, NY USA
7. Department of Radiology, Washington University School of Medicine, Saint Louis, MO USA
8. Department of Neurology, Washington University School of Medicine, Saint Louis, MO USA
9. Department of Neuroscience, Icahn School of Medicine at Mount Sinai, New York, NY USA
10. Dementia Research Centre, Department of Neurodegenerative Disease, UCL Institute of Neurology, London, UK
11. Department of Pathology and Immunology, Washington University School of Medicine, Saint Louis, MO USA
12. Department of Pathology and Laboratory Medicine, Indiana University School of Medicine, Indianapolis, IN USA
13. Centre of Excellence of Alzheimer's Disease Research and Care, School of Exercise, Biomedical and Health Sciences, Edith Cowan University, Perth, Australia
14. Center for Neuroimaging, Department of Radiology and Imaging Science, Indiana University School of Medicine, Indianapolis, IN USA
15. The Florey Institute, University of Melbourne, Parkville, Australia
16. Memory and Aging Center, Keck School of Medicine of University of Southern California, Los Angeles, CA USA
17. German Center for Neurodegenerative Diseases (DZNE) München and Tübingen and Department of Nuclear Medicine, Technische Universität München (TUM), Munich, Germany
18. German Center for Neurodegenerative Diseases (DZNE) and and Section for Dementia Research, Department of Cellular Neurology, Hertie Institute for Clinical Brain Research and Department of Psychiatry and Psychotherapy, University of Tübingen, Tübingen, Germany
19. Neuroscience Research Australia and University of New South Wales, Sydney, Australia
20. Center for Alzheimer Research and Treatment, Brigham and Women's Hospital and Massachusetts General Hospital, Boston, MA USA
21. Butler Hospital and Department of Neurology, Alpert Medical School, Brown University, Providence, RI USA
22. Department of Psychiatry, Alpert Medical School. Brown University, Providence, RI USA
23. Department of Radiology, Mayo Clinic, Rochester, MN USA

Accepted Article

This article is protected by copyright. All rights reserved.

24. Department of Radiology and Biomedical Imaging, Center for Imaging of Neurodegenerative Diseases, San Francisco Veterans Affairs Medical Center and Departments of Psychiatry, Radiology, Medicine, and Neurology, University of California at San Francisco, San Francisco, CA USA
25. Gertrude H. Sergievsky Center, College of Physicians and Surgeons, Columbia University, New York, NY USA

[¥]Authors contributed equally to this work

*Corresponding author:
Adam M. Brickman, PhD
Taub Institute for Research on Alzheimer's Disease and the Aging Brain
Department of Neurology
College of Physicians and Surgeons
Columbia University

630 West 168th Street
P&S Box 16
New York, NY 10032, USA
Email: amb2139@columbia.edu
Tel: +1 212 342 1348
Fax: +1 212 342 1838

Total word count: 3,035

Accepted Article

This article is protected by copyright. All rights reserved.

Abstract

Objective. White matter hyperintensities(WMH) are areas of increased signal on magnetic resonance imaging(MRI) scans that most commonly reflect small vessel cerebrovascular disease. Increased WMH volume is associated with risk and progression of Alzheimer's disease(AD). These observations are typically interpreted as evidence that vascular abnormalities play an additive, independent role contributing to symptom presentation, but not core features of AD. We examined the severity and distribution of WMH in presymptomatic *PSEN1*, *PSEN2*, and *APP* mutation carriers to determine the extent to which WMH manifest in individuals genetically-determined to develop AD.

Methods. The study comprised participants(n=299, age=39.03±10.13) from the Dominantly Inherited Alzheimer Network, including 184(61.5%) with a mutation that results in AD and 115(38.5%) first-degree relatives who were non-carrier controls. We calculated the estimated years from expected symptom onset(EYO) by subtracting the affected parent's symptom onset age from the participant's age. Baseline MRI data were analyzed for total and regional WMH. Mixed effects piecewise linear regression was used to examine WMH differences between carriers and non-carriers with respect to EYO.

Results. Mutation carriers had greater total WMH volumes, which appeared to increase approximately 6 years prior to expected symptom onset. The effects were most prominent for the parietal and occipital lobe, which showed divergent effects as early as 22 years prior to estimated onset.

Interpretation. Autosomal dominant AD is associated with increased WMH well before expected symptom onset. The findings suggest the possibility that WMH are a core feature of AD, a potential therapeutic target, and a factor that should be integrated into pathogenic models of the disease.

Accepted Article

This article is protected by copyright. All rights reserved.

Introduction

White matter hyperintensities (WMH), visualized as increased signal on T2-weighted magnetic resonance imaging (MRI) of the brain are common radiological features of aging. Previously thought to reflect benign changes in underlying tissue or radiographic artifacts, they have emerged as correlates of cognitive, functional, emotional, and motoric abnormalities that emerge in later life[1] and have been linked pathologically to small vessel cerebrovascular disease, including arteriosclerosis, demyelination and axonal loss due to ischemia or neuronal death, cerebral amyloid angiopathy, and microglia activation[2]. In recent years, there has been strong evidence that WMH are associated with the clinical risk and symptomatic course of late onset Alzheimer's disease (LOAD)[3]. Despite these consistent observations, white matter abnormalities are not included in current conceptual models of the pathogenesis and biological marker progression of LOAD (e.g., [4]). The debate on the extent to which WMH represent a core feature of LOAD can be summarized in two opposing views. On the one hand, because AD is defined pathologically by the presence of Aβ plaques with neuritic plaques and neurofibrillary tangles adding to the severity of the changes, white matter damage is considered a comorbidity that does not represent these pathologies. On the other hand, WMH predict the clinical onset and course of AD similarly to or better than other biological markers of AD[5, 6], may in part reflect vascular forms of AD pathology, there are viable biological models that implicate small vessel cerebrovascular disease in the deposition of primary AD pathology[7], and among individuals with late onset dementia, presence of multiple pathologies is more common than not [8-10].

The study of the emergence of WMH - - or any biological markers - - and their contributions to LOAD in humans is difficult because the ordering and timing of the biological changes that lead to dementia can occur up to decades before the onset of symptoms[4], which is typically the point when human studies of LOAD are conducted. White matter hyperintensity severity is also tightly linked to vascular risk factors

Accepted Article

This article is protected by copyright. All rights reserved.

and age[2], so determination of its contribution to late onset AD is potentially confounded by these factors. To overcome these issues, we turned to the landmark Dominantly Inherited Alzheimer Network (DIAN) study. The study enrolls individuals at 50% risk for autosomal dominant AD by virtue of having a first-degree relative with a pathogenic mutation in one of three AD-causing genes: amyloid precursor protein (*APP*), presenilin 1 (*PSEN1*), and presenilin 2 (*PSEN2*). Pathogenic mutations are virtually fully penetrant, leading to 100% probability that the mutation carrier will develop early onset AD. Although autosomal dominant forms of AD account for fewer than 1% of all AD cases, there is strong overlap in symptomatology with LOAD, and a recent critical DIAN study established that the order of biological changes begins with deposition of amyloid, followed by neurodegenerative changes (e.g., as indexed by levels of tau protein in the cerebrospinal fluid [CSF]), and cognitive decline [11]. Because the age at onset of clinical symptoms is highly heritable among individuals with autosomal dominant AD[12], parental age at onset can be used as a reliable estimate of clinical onset among asymptomatic mutation carriers. Here, we tested the hypothesis that WMH burden is elevated among mutation carriers and increases with greater temporal proximity to the estimated year of onset of clinical symptoms. Our goal was to determine definitively whether WMH are a core feature of AD. Given our previous observations of a WMH regional selectivity in LOAD, we also examined the regional distribution of WMH.

Methods

Overall design

The DIAN study (www.dian-info.org; NIA-U19-AG032438) is an international effort that includes sites in USA, UK, Germany, and Australia. The study recruits individuals from families with a known autosomal dominant mutation for AD, including *APP*, *PSEN1*, and *PSEN2*, irrespective of their own mutation status. As part of the DIAN Observational Study, participants receive a baseline assessment with sampling of blood and CSF, clinical assessment, neuropsychological evaluation, and neuroimaging, and are followed

Accepted Article

This article is protected by copyright. All rights reserved.

longitudinally with identical assessments. Full procedures for the study are described elsewhere[11, 13]. All study procedures received approval from each participating institution and all participants gave informed consent.

Clinical assessment

All evaluation procedures were conducted by individuals unaware of the mutation status of each participant. The clinical assessment included evaluation with the Clinical Dementia Rating scale (CDR)[14], physical and neurological examination, neuropsychological testing, and determination of the parental age at onset. Parental age at onset was determined with a semi-structured interview that assessed the age at which the affected parent began exhibiting signs of progressive cognitive decline [11]. Estimated years from expected symptom onset (EYO) were calculated as the difference between the participant's age and the parental age at onset[11]. This variable was established for all participants regardless of their own mutation status. Data included in the present study were a subset from Data Freeze 6 with available T2-weighted magnetic resonance imaging (MRI) scans. Remote or current history of hypertension, hypercholesterolemia, diabetes, and smoking ($\geq$ 100 cigarettes smoked in lifetime) was ascertained via interview and considered in secondary analyses.

Biochemical and genetic analysis

Cerebrospinal fluid was collected via lumbar puncture on each participant under fasting conditions[11]. Samples were shipped to the DIAN biomarker core laboratory and immunoassay (INNOTEST β-Amyloid$_{1-42}$ and INNO-BIA AlzBio3) was used to measure CSF concentrations of Aβ_{1-42} and phosphorylated tau (ptau181). All samples underwent quality control procedures[11]. Each participant's mutation status and *APOE* genotype was determined according to procedures in the published DIAN protocol[11, 13].

This article is protected by copyright. All rights reserved.

Accepted Article

Brain imaging

Participants received structural MRI. For the current study, we quantified WMH on T2-weighted fluid attenuated inversion recovery (FLAIR) structural MRI scans. Scan acquisition took place on pre-qualified 3T scanners at each site. Harmonization and quality assurance across platforms, sites, and acquisition times followed the Alzheimer's Disease Neuroimaging Initiative (ADNI) protocols[15]. The neuroimaging core laboratory reviewed each MRI scan to ensure compliance with the acquisition protocol and image quality. Standardized FLAIR sequences (TR:9000, TE:90, TI: 2500, voxel dimensions: 0.86 X 0.86 x 5.0 mm) were acquired as part of the DIAN MRI protocol. The FLAIR images were transferred to Columbia University for WMH quantification using procedures previously described[16]. Briefly, a study-specific intensity threshold was applied to each image to label voxels falling within the WMH intensity distribution. An expert operator reviewed and edited every image if necessary. A "lobar" atlas was co-registered linearly to each labeled FLAIR image to define WMH volumes in frontal, temporal, parietal, and occipital lobes. White matter hyperintensity volume was defined as the sum of the labeled voxels multiplied by voxel dimensions; regional volumes were calculated within each labeled lobar region-of-interest. In a random subset of 10 participants, test-retest reliability was greater than 0.98 for regional and total WMH volumes. All imaging analyses were completed without knowledge of mutation status and demographic and clinical data.

In a subset of participants, T2*-weighted MR images were analyzed at the Mayo Clinic (Rochester, MN) for presence of cerebral microbleeds. We operationally defined possible cerebral amyloid angiopathy (CAA) as the presence of at least one cerebral microbleed according to the Boston criteria[17]. We examined whether the presence of cerebral microbleeds mediated the hypothesized relationship between WMH and mutation status.

Statistical analysis

This article is protected by copyright. All rights reserved.

Accepted Article

Demographic and clinical variables were compared between mutation carriers and non-carriers with t-tests and Chi-squared analysis for continuous and categorical data, respectively. We explored the relationship between total WMH volume and CSF-derived AD biomarkers with Spearman's rank order correlations stratified by mutation status. To test whether WMH volume differed by mutation type, we used a general linear model that examined the interaction between Carrier Status (carrier vs. non-carrier) and familial Mutation Type (*PSEN1*, *PSEN2*, *APP*). We employed piecewise linear mixed effect regression with an inflection point as a parameter[18] to examine the total and regional WMH volumes with respect to estimated years from symptom onset, controlling for participant family as a random effect. The primary parameter of interest was the interaction between Mutation Status and EYO, which would demonstrate that WMH volume is increasing among mutation carriers at a rate that is greater than non-mutation carriers. The inclusion of the inflection point as an additional parameter, in the context of a significant interaction, tests whether there is a point within the time period at which at which the association between EYO and WMH volume begins to diverge between mutation carriers and non-carriers. The inflection point was selected based on Bayesian Information Criterion (BIC)[19]; we tested whether the inclusion of the inflection point significantly improved the model fit compared with the model without the inflection point with the likelihood ratio test (LRT)[20]. Overall model fits were also determined with the LRT. Similar analyses were run with CSF measures of $A\beta_{1-42}$ (a marker of β-amyloid), ptau181 (a presumed marker of neurofibrillary tangles), and the ratio of $A\beta_{1-42}$ to ptau181, in order to compare the timing and ordering among the biomarkers. Analyses involving WMH were also re-run controlling for ptau181 (Model 2) or $A\beta_{1-42}$ (Model 3). Analyses were re-run after the inclusion of participant age and APOE-ε4 status as additional covariates to ensure that the primary observations were not confounded by these factors. Similarly we compared vascular risk histories between mutation carriers and non-carriers and computed a vascular risk summary score by adding the dichotomous variables together. This score was considered as a covariate in subsequent analyses. For visualization,

Accepted Article

This article is protected by copyright. All rights reserved.

LOESS regression analysis[21] was conducted and the estimates and their 95% confidence limits were drawn. Statistical analyses were conducted with the use of the PROC MIXED and SGPLOT procedures in SAS software, version 9.3 (SAS Institute). We tested the differences in total and regional WMH volumes in individuals with CDR scores of 0 with a general linear model, adjusting for participant's age, to ensure that differences between groups were not related to the inclusion of symptomatic individuals. Prior to statistical analyses, total and regional WMH volumes underwent inverse hyperbolic transformation because the distributions of these variables were highly positively skewed[22].

Similar mixed effects piecewise linear regression and formal testing of mediation was used to examine differences between carriers and non-carriers in presence of cerebral microbleeds and to test the whether the association between WMH and mutation status is dependent on the presence of cerebral microbleeds.

Results

Data from 299 participants of the total DIAN cohort that had passed rigorous quality assurance for Data Freeze 6 were included in these analyses (see Table 1 for demographic, clinical, and biomarker data). There were 184 (61.5%) mutation carriers, including 141 (77%) *PSEN1*, 15 (8%) *PSEN2*, and 28 (15%) *APP* mutation carriers. Mutation carriers and non-carriers were almost identical in age, sex distribution, vascular risk factors, EYO, and frequency of APOE-ε4, but had a greater proportion of symptomatic individuals (i.e., CDR>0). Mutation carriers had greater total, temporal, parietal, and occipital WMH volumes than non-carriers; these differences between mutation carriers and non-carriers remained when restricting the sample to asymptomatic participants (i.e., CDR=0; $p<0.05$ for total and occipital lobe, $p=0.09$ for parietal lobe, $p=0.11$ for temporal lobe). Differences in WMH volume between mutation carriers and non-carriers were not driven by a single mutation type, as evidenced by a significant main effect of Carrier Status ($p<0.05$) for all regions apart from frontal lobe, and non-significant interactions ($p>0.05$) between Carrier Status and Mutation Type for all regions. As expected,

This article is protected by copyright. All rights reserved.

Accepted Article

mutation carriers had lower levels of $A\beta_{1-42}$ and higher levels of ptau181 compared with non-carriers; these differences remained ($p<0.001$) when restricting the sample to individuals with CDR scores of 0. Increased total WMH volume was associated with lower $A\beta_{1-42}$ levels in mutation carriers ($r=-0.190$, $p=0.01$) but not in non-carriers ($r=-0.053$, $p=0.623$; see Figure 1). White matter hyperintensity volume was not related to ptau181 levels in mutation carriers ($r=-0.090$, $p=0.162$) or in mutation non-carriers ($r=-0.025$, $p=0.813$). Descriptive statistics for WMH volume, including median, first quartile, third quartile, and interquartile range are presented in Table 2.

Results of the piecewise linear mixed effect analyses revealed a reliable increase in total WMH volume among mutation carriers (significant Mutation Status by EYO interactions) with an inflection point occurring approximately 6.6 years prior to estimated symptom onset (EYO-6.6; see Figure 2 and Supplementary Table). When we examined the regional distribution of WMH, significant effects emerged in the parietal and occipital lobes. For the parietal lobe, much like total WMH volume, the inflection point occurred approximately seven years prior to estimated symptom onset (EYO -7). For the occipital lobes, the inflection point occurred approximately 22 years prior to estimated symptom onset (EYO -22; see Figure 3). Cerebrospinal fluid levels of $A\beta_{1-42}$, ptau181, and $A\beta_{1-42}$ to ptau181 ratio levels appeared to diverge in mutation carriers approximately 30, 26, and 29 years prior to estimated symptom onset, respectively. Thus, in terms of ordering and staging, the results suggest that total WMH volumes are increased reliably after amyloid and tau abnormalities are detectable but prior to symptom onset. Regionally, posterior WMH volume increases in mutation carriers at about the same time that CSF ptau181 and CSF amyloid changes occur. When adjusting for CSF AD biomarkers, total WMH volumes remained significantly elevated in mutation carriers when controlling for ptau181 levels but not when controlling for $A\beta_{1-42}$ levels. Figure 4 displays representative examples of WMH in mutation carriers and non-carriers across three EYO time points. When all analyses were repeated with age and

Accepted Article

This article is protected by copyright. All rights reserved.

APOE-ε4 status as additional covariates (data not shown) none of the primary observations were altered and the additional covariate parameters were not statistically significant. Similarly, when the analyses were re-run with the vascular risk summary score none of the primary observations changed.

When we examined the potential contribution of CAA among a subset of participants (n=175), we found that mutation carriers were more likely to have cerebral microbleeds than non-carriers (20% vs. 6%, $p<0.05$) and individuals with microbleeds had higher WMH volume than those without ($p<0.05$). White matter hyperintensity volume was increased in mutation carriers, up to 20 years prior to EYO, after controlling for microbleed status. Total WMH also remained significantly elevated in mutation carriers even after exclusion of individuals with microbleeds from the study sample. Formal testing of mediation demonstrated that 21% of the association between mutation status and WMH was mediated by presence of microbleeds ($p=0.03$) but a significant direct effect of WMH remained ($p=0.02$) after controlling for presence of microbleeds.

Discussion

We found that total WMH volume is significantly elevated among individuals with autosomal dominant genetic mutations for AD approximately six years prior to their estimated age of symptom onset. When considered regionally, WMH volume distributed in posterior brain areas is selectively elevated among mutation carriers about 22 years prior to estimated symptom onset. Together with the previous studies that have implicated WMH, particularly in posterior regions, in risk and progression of clinical symptomatology of LOAD [16, 23], our study suggests that WMH are an important feature of AD. Because mutation carriers and non-carriers in the current study are relatively young, virtually identical demographically, and at identical risk for inheriting an autosomal dominant mutation by virtue of having a parent with a mutation, the findings provide strong evidence that WMH in this population do not reflect comorbidity or other pathophysiology but rather reflect primary pathogenic processes in AD. The

Accepted Article

This article is protected by copyright. All rights reserved.

results highlight the potential role of regionally distributed WMH in AD and point to new avenues of investigation for preventative or treatment strategies.

In the context of other AD biomarkers, WMH appear to emerge globally after measurable changes in CSF $A\beta_{1-42}$ and ptau181 but prior to symptom onset, although WMH distributed in posterior brain areas appear elevated at about the same time as tau and $A\beta_{1-42}$ differences. These findings should be interpreted in the context of wide confidence intervals, and therefore relatively lower reliability, related to the inflection point analyses. White matter hyperintensity volume correlated with CSF $A\beta_{1-42}$ but not ptau181, and when controlling for $A\beta_{1-42}$ in our primary analyses, elevation of WMH associated with mutation status was attenuated. These results first suggest that WMH and beta amyloid pathology share some degree of dependency. We[24] and others[25, 26] have shown previously that WMH volume and markers of fibrillar amyloid pathology are related to each other in the context of LOAD, though others have not[27]. This study confirms that the two biomarkers are related to each other in individuals with definite pre-clinical AD. Second, they suggest that WMH do not result primarily from tau-related neurodegeneration, although the extent to which WMH are related to axonal damage secondary to tau abnormalities cannot be ruled out entirely by these analyses. We showed in ADNI that WMH severity predicts future CSF tau increases and neurodegenerative changes but that CSF tau levels do not predict future WMH accumulation[28]. We found that CSF $A\beta_{1-42}$is levels appear to be initially higher followed by a rapid decline as a function of EYO in mutation carriers compared with non-carriers (see Figure 3), suggesting that $A\beta_{1-42}$ are abnormally elevated and begin to decline prior to increases in tau. It is important to note that because the analyses were cross-sectional, the determination of an inflection point was estimated and variable, and we were unable to model the subject-specific trajectories, which would require longitudinal data. Nonetheless, in all cases but one (the statistical model in which we controlled for $A\beta_{1-42}$, see Supplementary Table), inclusion of the inflection point significantly improved

Accepted Article

This article is protected by copyright. All rights reserved.

the model fit. Furthermore, our approach determined definitively that the relationship between estimated time to symptom onset and WMH volume differed between mutation carriers and non-carriers (i.e., significant Mutation Status by EYO interactions) and, much like previous work in DIAN [11], allowed us to compare the evolution of WMH compared with the other biological markers.

White matter hyperintensities are generally considered markers of small vessel cerebrovascular disease[29, 30], although it is important to point out that non-ischemic damage that causes increased fluid motion in discrete areas in the white matter can result in hyperintense signal. Pathogenic mechanisms are not known completely, but a recent genetic meta-analysis suggested a role of blood pressure regulation, Aβ-related neurotoxicity, neuroinflammation, and glial cell activation[31]. Pathological correlates, immunohistochemical, and gene expression studies suggest demyelination, axonal loss, gliosis, vacuolation, microglial activation, arteriolosclerosis, and blood brain barrier dysfunction are secondary to ischemic injury in areas appearing radiographically as WMH [2]. The pathophysiology of WMH is likely heterogeneous and only one study to our knowledge has examined the pathological correlates of WMH among individuals with autosomal dominant forms of AD, in whom the mediators of WMH might differ somewhat[32]. In that report, WMH burden correlated with the severity of cerebral amyloid angiopathy in the temporal lobes, leptomeningeal blood vessel diameter, and lower density of CD68-positive microglia in the parietal lobes among 10 individuals with *PSEN1* mutations. Given the propensity for a posterior distribution of WMH we found in mutation carriers, cerebral amyloid angiopathy, which also tends to be distributed in posterior brain regions, is present among individuals with autosomal dominant forms of AD years before symptoms onset, and correlates with severity of WMH[33], may be one mediating factor in these observations. Similarly, one previous report suggests that the WMH severity correlates with severity of fibrillar forms of amyloid pathology among individuals with CAA but not LOAD[34], again suggesting an influence of CAA on the observed relationship between WMH

This article is protected by copyright. All rights reserved.

Accepted Article

volume and $A\beta_{1-42}$ levels, and we could speculate that CAA may be one causative factor in the parenchymal deposition of Aβ. Although in the current study there was some co-dependency between WMH and presence of at least one cerebral microbleed, the observed increases in WMH among mutation carriers did not appear to be fully mediated by this marker of cerebral amyloid angiopathy. Loss of axons, myelin pallor, and diffuse Aβ has also been observed pathologically in the white matter of patients with autosomal dominant AD and LOAD and in animal models of the disease[35-38]. Alzheimer's-related failure of the axonal machinery due to mitochondrial dysfunction, white matter astroglial proliferation, venous collagenosis, and damage to oligodendrocytes and their progenitor cells are other possible pathological correlates of our results[36, 39-42]. Clearly more work relating radiological white matter abnormalities to pathological phenomena is necessary.

White matter hyperintensities are quite common in normal aging[43] and have been implicated in non-Alzheimer's forms of cognitive impairment and dementia[44]. Thus, the question of the extent to which WMH represent a specific biomarker for AD or for its clinical instantiation is valid and consistent with the conceptualization of other AD biomarkers. For example, increased beta amyloid pathology is observed in up to 40% of older individuals with no evidence of dementia [45, 46]; tau pathology is common in aging, in several neurodegenerative diseases, and in chronic traumatic brain injury [47-49], albeit with differing regional patterns across conditions; and regional atrophy is characteristic of LOAD [50], but is also common in normal aging [51]. Our observations, together with previous work that has implicated WMH in late onset AD, suggest the possibility that WMH could be incorporated more formally into proposed hypothetical models of disease pathogenesis, such as those proposed by Jack and colleagues[4]. The definitive relationship we observed between increased WMH and autosomal dominant forms of AD should motivate continued research on the involvement of white matter abnormalities with the disease, including examination of mechanistic interactions with other putative AD biomarkers.

Accepted Article

This article is protected by copyright. All rights reserved.

Acknowledgments

Funding. NIH/NIA U19 AG032438, NIHR Queen Square Dementia BRU, Seonjoo Lee is supported by NIH/NIA AG051348, German Center for Neurodegenerative Diseases (DZNE), Natalie Ryan is supported by a Brain Exit Foundation Fellowship. Work partially supported by the NIHR Queen Square Dementia BRU.

Author contributions

Conception and design of the study: SL, FV, MEZ, GT, TLSB, RJB, JCM, RM, AMB

Acquisition/analysis of data: SL, AN, GT, TLSB, DSM, AMF, AG, NCF, NJC, DMH, VB, BG, EM, RNM, AJS, CLM, JMR, NSR, SF, CL, PRS, RAS, SS, SC, CJ, MW, RJB, JCM, RM, AMB

Drafting manuscript or figures: SL, FV, MEZ, GT, AMB

Potential conflicts of interest

SL, FV, MEZ, AN, GT, TLSB, DSM, AF, AG, NJC, DMH, VB, BG, EM, RNM, AJS, CLM, JMR, NR, SF, CL, PRS, SS, SC, CJ, RJB, JCM, RM, and AMB have no relevant conflicts of interest

NF consults for Eli Lilly, Novartis, Sanofi, Roche, and GSK, which may conduct trials in autosomal dominant AD

RAS receives research support from Eli Lilly which manufactures solanezumab, being studied for the treatment of Alzheimer's disease in the DIAN Study, and from Avid, who manufactures florbetapir, a PET tracer to detect amyloid, that is being used in the DIAN Study.

MW provides consulting to Eli Lilly, which makes an amyloid PET ligand. Eli Lilly is testing anti-amyloid treatments for Alzheimer's disease.

Accepted Article

This article is protected by copyright. All rights reserved.

References

1. Debette S, Markus HS. The clinical importance of white matter hyperintensities on brain magnetic resonance imaging: systematic review and meta-analysis. BMJ. 2010;341:c3666.

2. Wardlaw JM, Valdes Hernandez MC, Munoz-Maniega S. What are White Matter Hyperintensities Made of? Relevance to Vascular Cognitive Impairment. J Am Heart Assoc. 2015;4(6).

3. Brickman AM. Contemplating Alzheimer's disease and the contribution of white matter hyperintensities. Curr Neurol Neurosci Rep. 2013 Dec;13(12):415.

4. Jack CR, Jr., Knopman DS, Jagust WJ, et al. Tracking pathophysiological processes in Alzheimer's disease: an updated hypothetical model of dynamic biomarkers. Lancet Neurol. 2013 Feb;12(2):207-16.

5. Lindemer ER, Salat DH, Smith EE, Nguyen K, Fischl B, Greve DN. White matter signal abnormality quality differentiates mild cognitive impairment that converts to Alzheimer's disease from nonconverters. Neurobiol Aging. 2015 May 28.

6. Brickman AM, Provenzano FA, Muraskin J, et al. Regional white matter hyperintensity volume, not hippocampal atrophy, predicts incident Alzheimer disease in the community. Arch Neurol. 2012 Dec;69(12):1621-7.

7. Zlokovic BV. Neurovascular pathways to neurodegeneration in Alzheimer's disease and other disorders. Nat Rev Neurosci. 2011;12(12):723-38.

8. White L. Brain lesions at autopsy in older Japanese-American men as related to cognitive impairment and dementia in the final years of life: a summary report from the Honolulu-Asia aging study. J Alzheimers Dis. 2009;18(3):713-25.

9. Schneider JA, Arvanitakis Z, Bang W, Bennett DA. Mixed brain pathologies account for most dementia cases in community-dwelling older persons. Neurology. 2007 Dec 11;69(24):2197-204.

Accepted Article

This article is protected by copyright. All rights reserved.

10. Cairns NJ, Perrin RJ, Franklin EE, et al. Neuropathologic assessment of participants in two multi-center longitudinal observational studies: The Alzheimer Disease Neuroimaging Initiative (ADNI) and the Dominantly Inherited Alzheimer Network (DIAN). Neuropathology. 2015 Aug;35(4):390-400.

11. Bateman RJ, Xiong C, Benzinger TL, et al. Clinical and biomarker changes in dominantly inherited Alzheimer's disease. N Engl J Med. 2012 Aug 30;367(9):795-804.

12. Ryman DC, Acosta-Baena N, Aisen PS, et al. Symptom onset in autosomal dominant Alzheimer disease: a systematic review and meta-analysis. Neurology. 2014 Jul 15;83(3):253-60.

13. Morris JC, Aisen PS, Bateman RJ, et al. Developing an international network for Alzheimer research: The Dominantly Inherited Alzheimer Network. Clin Investig (Lond). 2012 Oct 1;2(10):975-84.

14. Morris JC, Ernesto C, Schafer K, et al. Clinical dementia rating training and reliability in multicenter studies: the Alzheimer's Disease Cooperative Study experience. Neurology. 1997 Jun;48(6):1508-10.

15. Jack CR, Jr., Bernstein MA, Borowski BJ, et al. Update on the magnetic resonance imaging core of the Alzheimer's disease neuroimaging initiative. Alzheimers Dement. 2010 May;6(3):212-20.

16. Brickman AM, Zahodne LB, Guzman VA, et al. Reconsidering harbingers of dementia: progression of parietal lobe white matter hyperintensities predicts Alzheimer's disease incidence. Neurobiol Aging. 2015 Jan;36(1):27-32.

17. Knudsen KA, Rosand J, Karluk D, Greenberg SM. Clinical diagnosis of cerebral amyloid angiopathy: validation of the Boston criteria. Neurology. 2001;56(4):537-9.

18. McZgee VE, Carleton WT. Piecewise regression. Journal of the American Statistical Association. 1970;65(331):1109-24.

19. Kim HJ, Yu B, Feuer EJ. SELECTING THE NUMBER OF CHANGE-POINTS IN SEGMENTED LINE REGRESSION. Stat Sin. 2009 May 1;19(2):597-609.

This article is protected by copyright. All rights reserved.

Accepted Article

20. Piepho HP, Ogutu JO. Inference for the break point in segmented regression with application to longitudinal data. Biometrical Journal. 2003;45(5):591-601.

21. Cleveland WS. Robust locally-weighted regression and smoothing scatterplots. Journal of the American Statistical Association. 1979;74:829-36.

22. Burbridge JB, Magee L, Robb AL. Alternative transformations to handle extreme values of the dependent variable. Journal of the American Statistical Association. 1988;83(401):123-7.

23. Prins ND, Scheltens P. White matter hyperintensities, cognitive impairment and dementia: an update. Nat Rev Neurol. 2015 Mar;11(3):157-65.

24. Brickman AM, Guzman VA, Gonzalez-Castellon M, et al. Cerebral autoregulation, beta amyloid, and white matter hyperintensities are interrelated. Neurosci Lett. 2015 Apr 10;592:54-8.

25. Grimmer T, Faust M, Auer F, et al. White matter hyperintensities predict amyloid increase in Alzheimer's disease. Neurobiol Aging. 2012 Dec;33(12):2766-73.

26. Zhou Y, Yu F, Duong TQ. White matter lesion load is associated with resting state functional MRI activity and amyloid PET but not FDG in mild cognitive impairment and early Alzheimer's disease patients. J Magn Reson Imaging. 2015 Jan;41(1):102-9.

27. Vemuri P, Lesnick TG, Przybelski SA, et al. Vascular and amyloid pathologies are independent predictors of cognitive decline in normal elderly. Brain. 2015 Mar;138(Pt 3):761-71.

28. Tosto G, Zimmerman ME, Hamilton JL, Carmichael OT, Brickman AM, Alzheimer's Disease Neuroimaging I. The effect of white matter hyperintensities on neurodegeneration in mild cognitive impairment. Alzheimers Dement. 2015 Jun 13.

29. Erten-Lyons D, Woltjer R, Kaye J, et al. Neuropathologic basis of white matter hyperintensity accumulation with advanced age. Neurology. 2013 September 10, 2013;81(11):977-83.

30. Shim YS, Yang DW, Roe CM, et al. Pathological correlates of white matter hyperintensities on magnetic resonance imaging. Dement Geriatr Cogn Disord. 2015;39(1-2):92-104.

Accepted Article

This article is protected by copyright. All rights reserved.

31. Verhaaren BF, Debette S, Bis JC, et al. Multiethnic genome-wide association study of cerebral white matter hyperintensities on MRI. Circ Cardiovasc Genet. 2015 Apr;8(2):398-409.

32. Ryan NS, Biessels GJ, Kim L, et al. Genetic determinants of white matter hyperintensities and amyloid angiopathy in familial Alzheimer's disease. Neurobiol Aging. in press.

33. Thanprasertsuk S, Martinez-Ramirez S, Pontes-Neto OM, et al. Posterior white matter disease distribution as a predictor of amyloid angiopathy. Neurology. 2014 Aug 26;83(9):794-800.

34. Gurol ME, Viswanathan A, Gidicsin C, et al. Cerebral amyloid angiopathy burden associated with leukoaraiosis: a positron emission tomography/magnetic resonance imaging study. Ann Neurol. 2013 Apr;73(4):529-36.

35. Takao M, Ghetti B, Murrell JR, et al. Ectopic white matter neurons, a developmental abnormality that may be caused by the PSEN1 S169L mutation in a case of familial AD with myoclonus and seizures. J Neuropathol Exp Neurol. 2001 Dec;60(12):1137-52.

36. Sun SW, Song SK, Harms MP, et al. Detection of age-dependent brain injury in a mouse model of brain amyloidosis associated with Alzheimer's disease using magnetic resonance diffusion tensor imaging. Exp Neurol. 2005 Jan;191(1):77-85.

37. Collins-Praino L, Francis Y, Wiegman AF, et al. Soluble amyloid beta levels are elevated in the white matter of Alzheimer's patietns, independent of cortical plaque burden. Acta Neuropathologica Communications. 2014;2:83.

38. Brendza RP, O'Brien C, Simmons K, et al. PDAPP; YFP double transgenic mice: a tool to study amyloid-beta associated changes in axonal, dendritic, and synaptic structures. J Comp Neurol. 2003 Feb 17;456(4):375-83.

39. Behrendt G, Baer K, Buffo A, et al. Dynamic changes in myelin aberrations and oligodendrocyte generation in chronic amyloidosis in mice and men. Glia. 2013 Feb;61(2):273-86.

Accepted Article

This article is protected by copyright. All rights reserved.

40. Leuba G, Kraftsik R. Visual cortex in Alzheimer's disease: occurrence of neuronal death and glial proliferation, and correlation with pathological hallmarks. Neurobiol Aging. 1994 Jan-Feb;15(1):29-43.

41. Reddy PH. Abnormal tau, mitochondrial dysfunction, impaired axonal transport of mitochondria, and synaptic deprivation in Alzheimer's disease. Brain Res. 2011;1415:136-48.

42. Pantoni L. Cerebral small vessel disease: from pathogenesis and clinical characteristics to therapeutic challenges. The Lancet Neurology. 2010 7//;9(7):689-701.

43. DeCarli C, Massaro J, Harvey D, et al. Measures of brain morphology and infarction in the framingham heart study: establishing what is normal. Neurobiol Aging. 2005 Apr;26(4):491-510.

44. Gorelick PB, Scuteri A, Black SE, et al. Vascular contributions to cognitive impairment and dementia: a statement for healthcare professionals from the american heart association/american stroke association. Stroke. 2011 Sep;42(9):2672-713.

45. Bennett DA, Schneider JA, Arvanitakis Z, et al. Neuropathology of older persons without cognitive impairment from two community-based studies. Neurology. 2006 Jun 27;66(12):1837-44.

46. Aizenstein HJ, Nebes RD, Saxton JA, et al. Frequent amyloid deposition without significant cognitive impairment among the elderly. Arch Neurol. 2008 Nov;65(11):1509-17.

47. DeKosky ST, Blennow K, Ikonomovic MD, Gandy S. Acute and chronic traumatic encephalopathies: pathogenesis and biomarkers. Nat Rev Neurol. 2013 04//print;9(4):192-200.

48. Crary JF, Trojanowski JQ, Schneider JA, et al. Primary age-related tauopathy (PART): a common pathology associated with human aging. Acta Neuropathol. 2014 Dec;128(6):755-66.

49. McKee AC, Stein TD, Kiernan PT, Alvarez VE. The neuropathology of chronic traumatic encephalopathy. Brain Pathol. 2015 May;25(3):350-64.

50. Jack CR, Jr., Petersen RC, O'Brien PC, Tangalos EG. MR-based hippocampal volumetry in the diagnosis of Alzheimer's disease. Neurology. 1992 Jan;42(1):183-8.

Accepted Article

This article is protected by copyright. All rights reserved.

51. Raz N, Lindenberger U, Rodrigue KM, et al. Regional Brain Changes in Aging Healthy Adults: General Trends, Individual Differences and Modifiers. Cereb Cortex. 2005 November 1, 2005;15(11):1676-89.

Accepted Article

This article is protected by copyright. All rights reserved.

Table 1. Demographic, clinical, and biomarker data in mutation carriers and non-carriers.

		Mutation non-carriers	Mutation carriers	Total sample	Statistic
N		115	184	299	
Age, mean years ± SD		39.95 ± 9.93	39.09 ± 10.29	39.03 ± 10.13	t=0.115, p=0.908
EYO, mean years ± SD		-7.86 ± 11.57	-7.39 ± 9.51	-7.57 ± 10.34	t=0.385, p=0.703
Women, n(%)		65 (56.5%)	104 (56.5%)	169 (56.5%)	χ^2=0.00, p=1.00
Vascular factors	Hypertension	17 (15%)	18 (10%)	35 (12%)	χ^2=1.3, p=0.26
	Hypercholesterolemia	20 (17%)	28 (15%)	48 (16%)	χ^2=0.09, p=0.77
	Diabetes	2 (1.7%)	3 (1.6%)	5 (1.7%)	χ^2=0.005, p=0.94
	Smoking	49 (43%)	74 (40%)	123 (41%)	χ^2=0.08, p=0.77
CDR	0	107 (93%)	114 (62%)	221 (74%)	χ^2=37.31, p<0.001
	0.5	8 (7%)	43 (23%)	51 (17%)	
	1	0 (0%)	20 (11%)	20 (6.67%)	
	2	0 (0%)	5 (3%)	5 (1.67%)	
	3	0 (0%)	2 (1%)	2 (0.67%)	
APOE-ε4+		33 (29%)	56 (30.4%)	89 (30%)	χ^2=0.102, p=0.749
WMH, mean IHS ± SD[§]	Frontal	0.15 ± 0.34	0.47 ± 2.92	0.35 ± 2.30	t=1.44, p=0.151
	Temporal	0.02 ± 0.11	0.12 ± 0.48	0.08 ± 0.39	t=2.62, p=0.009
	Parietal	0.06 ± 0.25	0.41 ± 2.29	0.27 ± 1.811	t=2.05, p=0.042
	Occipital	0.09 ± 0.16	0.33 ± 0.77	0.24 ± 0.62	t=4.08, p<0.001
	Total	0.39 ± 0.73	1.42 ± 6.02	1.03 ± 4.77	t=2.29, p=0.023
CSF A$\beta_{1\text{-}42}$[*§]		411.40 ± 113.49	304.50 ± 156.85	343.93 ± 151.25	t=6.14, p<0.001
CSF ptau181[¥§]		29.93 ± 10.18	65.58 ± 37.79	52.41 ± 35.12	t=11.14, p<0.001
CSF A$\beta_{1\text{-}42}$:tau ratio		8.123 ± 4.23	4.26 ± 4.02	5.68 ± 4.49	t=7.11, p<0.001

[§]Equal variances not assumed because Levene's Test for Equality of Variances was significant (p<0.01)

[*]Available for n=244

[¥]Available for n=249

Accepted Article

This article is protected by copyright. All rights reserved.

EYO=estimated years to symptom onset, CDR=Clinical Dementia Rating scale, WMH=white matter hyperintensities, IHS=inverse hyperbolic sine

Accepted Article

This article is protected by copyright. All rights reserved.

Table 2. Descriptive statistics of WMH volume (in cm^3), including median, first quartile (Q1), third quartile (Q3), and interquartile range for tight bands of participants defined by estimated years to symptom onset and stratified by mutation status.

	Mutation non-carrier					Mutation carrier					Total				
EYO	**N**	**Med**	**Q1**	**Q3**	**IQR**	**N**	**Med**	**Q1**	**Q3**	**IQR**	**N**	**Med**	**Q1**	**Q3**	**IQR**
-30 to -20 y	13	0.19	0.04	0.44	0.40	18	0.41	0.19	0.72	0.54	31	0.24	0.04	0.72	0.68
-20 to -10 y	40	0.35	0.05	0.79	0.74	52	0.29	0.05	0.81	0.76	92	0.34	0.05	0.80	0.75
-10 to 0 y	36	0.23	0.05	0.75	0.70	73	0.37	0.09	1.01	0.91	109	0.32	0.05	0.97	0.92
0 to 10 y	15	0.08	0.00	0.36	0.36	35	0.43	0.00	1.93	1.93	50	0.29	0.00	1.10	1.10
10 to 21 y	11	0.27	0.00	0.48	0.48	6	0.55	0.13	2.12	1.99	17	0.27	0.10	0.51	0.41
Total	115	0.24	0.04	0.66	0.62	184	0.37	0.07	0.97	0.90	299	0.31	0.05	0.89	0.84

Accepted Article

This article is protected by copyright. All rights reserved.

Supplementary Table. Parameter estimates for primary analyses. The top panel shows the results for models that examined total WMH volume. Model 1 is adjusted for age and *APOE*-ε4 status. Model 2 is adjusted for age, *APOE*-ε4, and CSF ptau181 levels. Model 3 is adjusted for CSF $A\beta_{42}$ levels. The bottom 3 panels show the results from the regional WMH analyses and from the analyses that examined CSF tau and CSF $A\beta_{42}$ levels as outcomes. For all models, overall model fits were significant (LRT test, p's <0.0001).

	Total WMH											
Parameter	Beta		95% CI		Beta		95% CI		Beta		95% CI	
Intercept	0.404	**	0.198	0.610	0.511	**	0.237	0.784	0.754	***	0.4	1.1
EYO	0.003		-0.007	0.012	0.096		-0.193	0.385	0.081		-0.1	0.3
Mutation status (carrier=1)	0.144		-0.037	0.325	0.001		-0.011	0.014	0.001		0.0	0.0
EYO x Mutation status	0.028	*	0.002	0.054	0.022	*	0.002	0.041	0.011		0.0	0.0
Inflection point	-6.6		-0.1	22.8	-19.0		12.9	27.6	-3.0		-21.0	30.0
LRT test (p-value)	0.03				0.03				0.48			
CSF ptau181					-0.004	*	-0.007	0.000				
CSF Aβ42									-0.001	*	-0.001	0.000
	Frontal Lobe WMH				Temporal Lobe WMH				Parietal Lobe WMH			
Intercept	0.168	**	0.056	0.279	0.047		-0.017	0.110	0.087		-0.032	0.206
EYO	0.001		-0.004	0.006	0.002		-0.001	0.005	0.003		-0.003	0.009
Mutation status (carrier=1)	0.027		-0.069	0.123	0.052	.	-0.004	0.108	0.051		-0.060	0.163
EYO x Mutation status	0.021	*	0.003	0.039	0.015	*	0.002	0.027	0.018	*	0.002	0.033
Inflection point	-3.0		-0.2	14.2	-1.3		-1.5	6.0	-7.0		-0.1	26.1
LRT test (p-value)	0.02				0.02				0.03			
	Occipital Lobe WMH				CSF pTAU181				CSF Aβ42			
Intercept	0.090		-0.018	0.197	34.707	***	25.578	43.835	439.490	***	395.260	483.720
EYO	0.002		-0.004	0.007	0.078		-0.384	0.540	1.354		-0.898	3.606
Mutation status (carrier=1)	0.056		-0.085	0.196	-2.942		-16.123	10.239	100.050	**	25.506	174.594
EYO x Mutation status	0.008	.	0.000	0.016	1.945	***	1.327	2.562	-9.619	***	-12.608	-6.630
Inflection point	-22.0		-21.0	30.0	-26.0		-21.0	30.0	-30.1		-21.0	30.0
LRT test (p-value)	0.05				<0.001				<0.001			
	CSF Aβ42/tau ratio											
Intercept	9.127	***	7.508	10.745								
EYO	-0.037		-0.099	0.026								
Mutation status (carrier=1)	-0.239		-2.142	1.665								
EYO x Mutation status	-0.176	***	-0.256	-0.096								

Accepted Article

John Wiley & Sons

This article is protected by copyright. All rights reserved.

Inflection point	-28.5	-21.0	-30.0		
LRT test (p-value)	<0.001				

. <0.1, *<0.05, **<0.01, ***<0.0001. #Likelihood ratio test (LRT) compared to the model without an inflection point.

Accepted Article

This article is protected by copyright. All rights reserved.

Figure 1. Correlation between total WMH volume and $A\beta_{1-42}$, plotted separately for mutation carriers and non-carriers. The relationship was significant (r=-0.26, p=0.0012) for carriers but not for non-carriers (r=-0.053, p=0.623). Shaded areas represent 95% confidence intervals. IHS=inverse hyperbolic sine transformation.

Accepted Article

This article is protected by copyright. All rights reserved.

Figure 2. Association between estimated year from symptom onset and total WMH volume in mutation carriers and non-carriers. Mutation carriers had greater total WMH volume; differences in WMH volume between groups began increasing systematically approximately 6.6 years prior to estimated symptom onset (inflection point: -6.6 EYO, indicated by arrow on x-axis). Shaded areas represent 95% confidence intervals. Arrow indicates the inflection point in the analysis. IHS=inverse hyperbolic sine transformation.

Accepted Article

This article is protected by copyright. All rights reserved.

Figure 3. Association between estimated year from symptom onset and regional WMH volumes and AD biomarkers in mutation carriers and non-carriers. In all cases, mutation carriers had more severe biomarker burden; the point at which differences between groups begin to increase systematically (i.e., inflection point) is indicated by an arrow on the x-axis. A: frontal lobe WMH volume (inflection point=-3.0 EYO); B: temporal lobe WMH volume (inflection point=-1.3 EYO); C: parietal lobe WMH volume (inflection point=-7.0 EYO); D: occipital lobe WMH volume (inflection point=-22.0 EYO); E: $A\beta_{42}$ (inflection point=-30.1 EYO); F: ptau181 (inflection point=-26.0 EYO). Shaded areas represent 95% confidence intervals. IHS=inverse hyperbolic sine transformation.

Accepted Article

This article is protected by copyright. All rights reserved.

Figure 4. Examples of WMH distribution in mutation carriers (upper row) and non-carriers (lower row) across three EYO time points. The top row displays examples of T2-weighted FLAIR MRI scans from three mutation carriers at varying estimated years from symptom onset. The bottom row displays examples of MRI scans from non-carriers matched for estimated years from symptom onset (based on parental age of onset). All participants displayed in this figure had CDR scores of 0 at the time of MRI scan.

Accepted Article

This article is protected by copyright. All rights reserved.

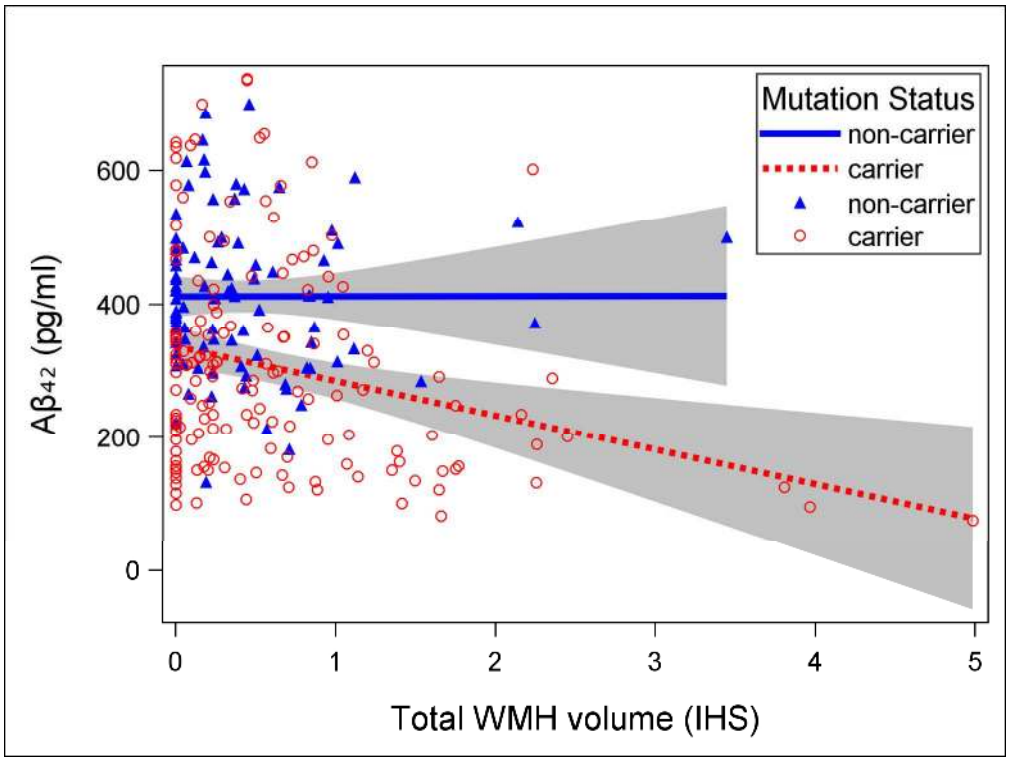

Figure 1. Correlation between total WMH volume and Aβ1-42, plotted separately for mutation carriers and non-carriers. The relationship was significant (r=-0.26, p=0.0012) for carriers but not for non-carriers (r=-0.053, p=0.623). Shaded areas represent 95% confidence intervals. IHS=inverse hyperbolic sine transformation.

Accep

This article is protected by copyright. All rights reserved.

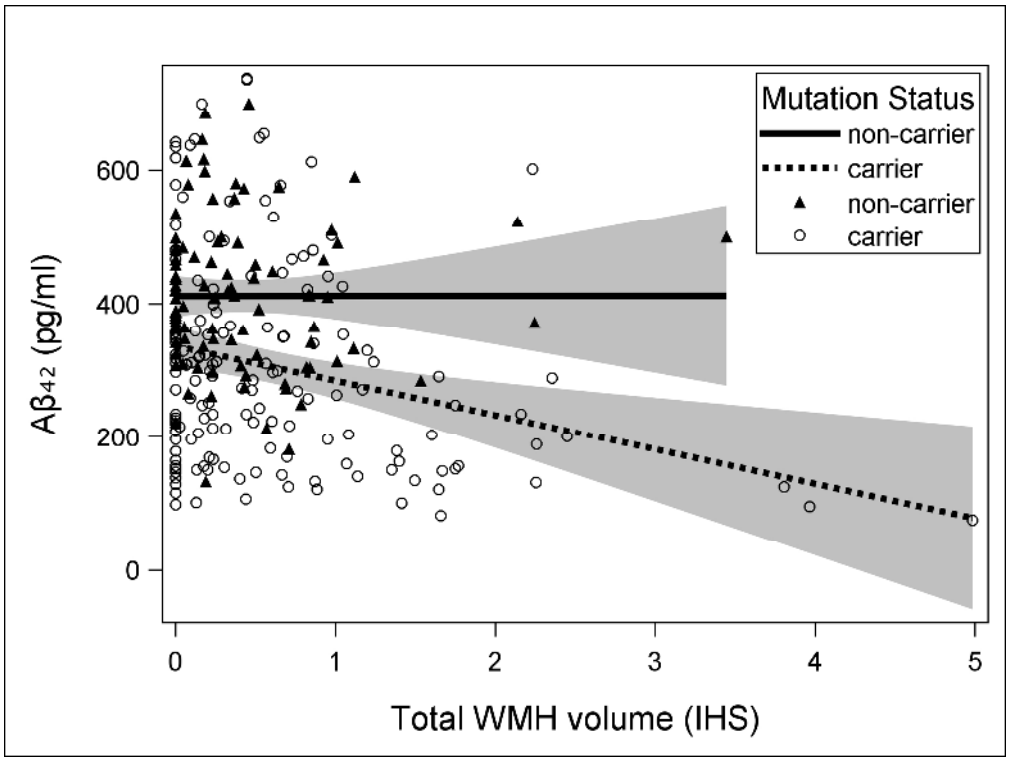

Figure 1. Correlation between total WMH volume and Aβ1-42, plotted separately for mutation carriers and non-carriers. The relationship was significant (r=-0.26, p=0.0012) for carriers but not for non-carriers (r=-0.053, p=0.623). Shaded areas represent 95% confidence intervals. IHS=inverse hyperbolic sine transformation.

Accep

This article is protected by copyright. All rights reserved.

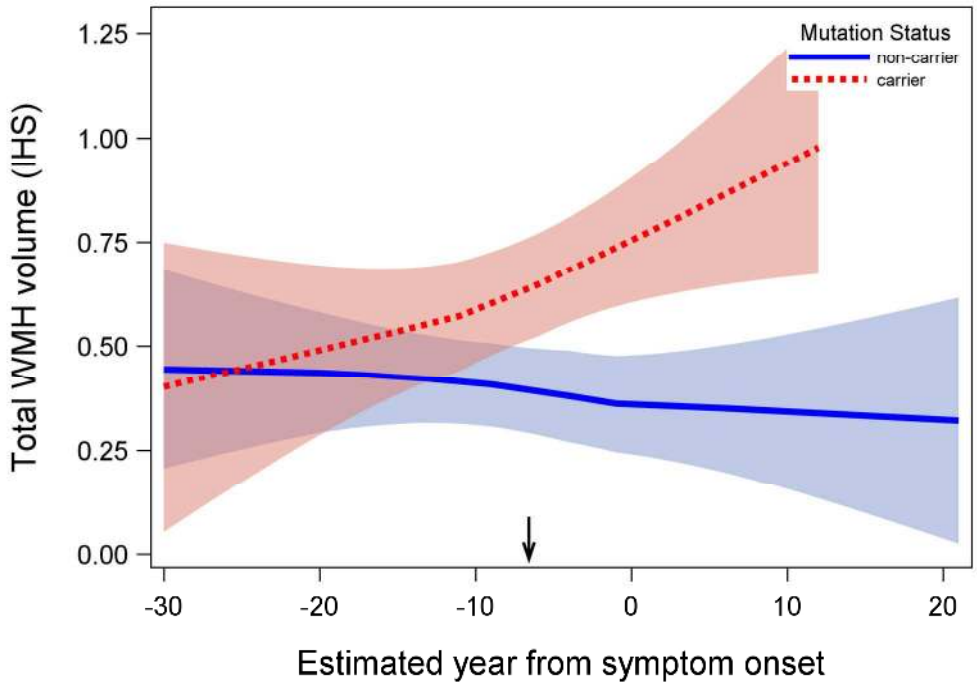

Figure 2. Association between estimated year from symptom onset and total WMH volume in mutation carriers and non-carriers. Mutation carriers had greater total WMH volume; differences in WMH volume between groups began increasing systematically approximately 6.6 years prior to estimated symptom onset (inflection point: -6.6 EYO, indicated by arrow on x-axis). Shaded areas represent 95% confidence intervals. Arrow indicates the inflection point in the analysis. IHS=inverse hyperbolic sine transformation.

Accepted

This article is protected by copyright. All rights reserved.

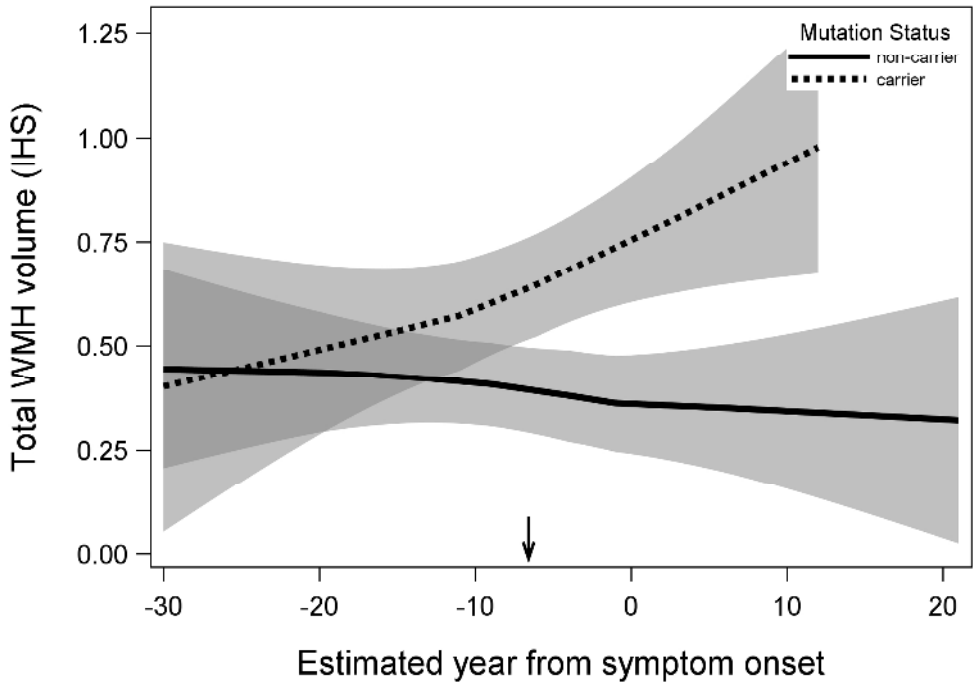

Figure 2. Association between estimated year from symptom onset and total WMH volume in mutation carriers and non-carriers. Mutation carriers had greater total WMH volume; differences in WMH volume between groups began increasing systematically approximately 6.6 years prior to estimated symptom onset (inflection point: -6.6 EYO, indicated by arrow on x-axis). Shaded areas represent 95% confidence intervals. Arrow indicates the inflection point in the analysis. IHS=inverse hyperbolic sine transformation.

Accepted

This article is protected by copyright. All rights reserved.

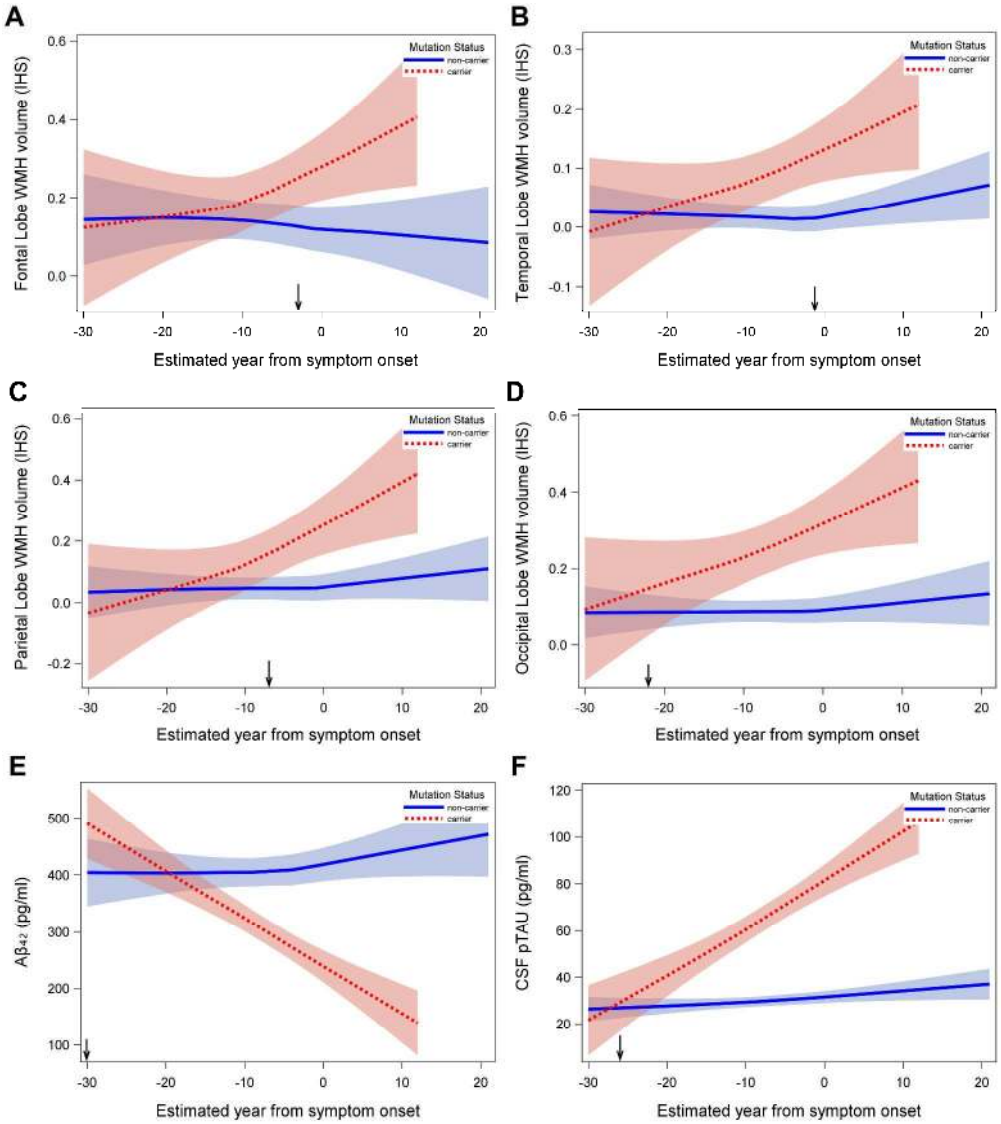

Figure 3. Association between estimated year from symptom onset and regional WMH volumes and AD biomarkers in mutation carriers and non-carriers. In all cases, mutation carriers had more severe biomarker burden; the point at which differences between groups begin to increase systematically (i.e., inflection point) is indicated by an arrow on the x-axis. A: frontal lobe WMH volume (inflection point=-3.0 EYO); B: temporal lobe WMH volume (inflection point=-1.3 EYO); C: parietal lobe WMH volume (inflection point=-7.0 EYO); D: occipital lobe WMH volume (inflection point=-22.0 EYO); E: Aβ42 (inflection point=-30.1 EYO); F: ptau181 (inflection point=-26.0 EYO). Shaded areas represent 95% confidence intervals. IHS=inverse hyperbolic sine transformation.

This article is protected by copyright. All rights reserved.

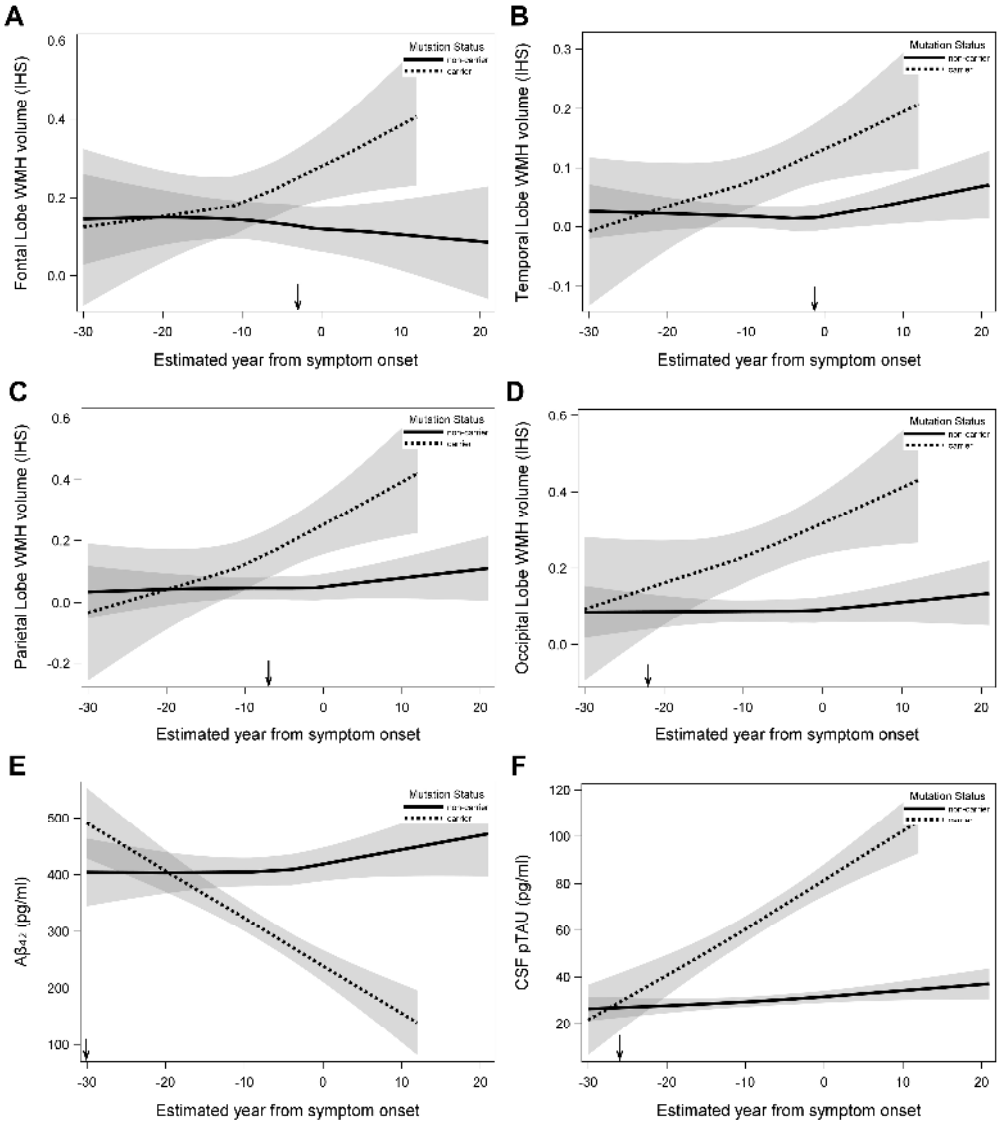

Figure 3. Association between estimated year from symptom onset and regional WMH volumes and AD biomarkers in mutation carriers and non-carriers. In all cases, mutation carriers had more severe biomarker burden; the point at which differences between groups begin to increase systematically (i.e., inflection point) is indicated by an arrow on the x-axis. A: frontal lobe WMH volume (inflection point=-3.0 EYO); B: temporal lobe WMH volume (inflection point=-1.3 EYO); C: parietal lobe WMH volume (inflection point=-7.0 EYO); D: occipital lobe WMH volume (inflection point=-22.0 EYO); E: Aβ42 (inflection point=-30.1 EYO); F: ptau181 (inflection point=-26.0 EYO). Shaded areas represent 95% confidence intervals. IHS=inverse hyperbolic sine transformation.

This article is protected by copyright. All rights reserved.

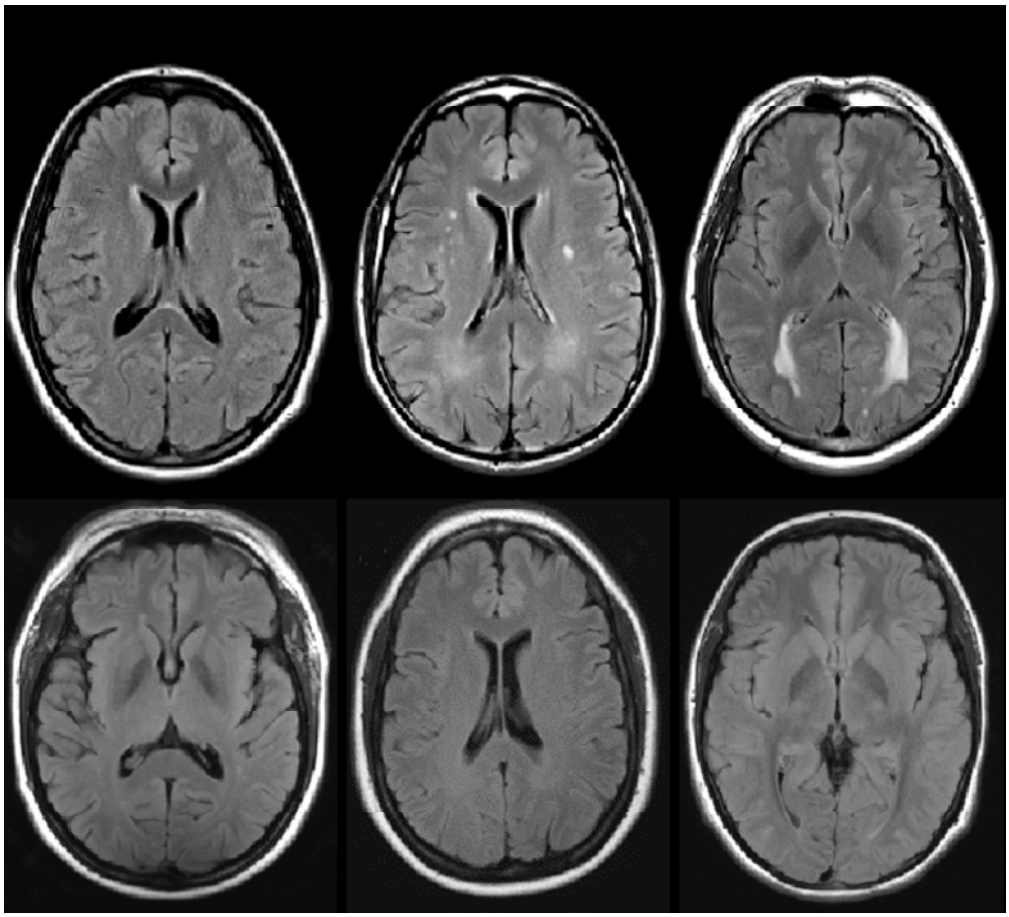

Figure 4. Examples of WMH distribution in mutation carriers (upper row) and non-carriers (lower row) across three EYO time points. The top row displays examples of T2-weighted FLAIR MRI scans from three mutation carriers at varying estimated years from symptom onset. The bottom row displays examples of MRI scans from non-carriers matched for estimated years from symptom onset (based on parental age of onset). All participants displayed in this figure had CDR scores of 0 at the time of MRI scan.
181x164mm (150 x 150 DPI)

Acc

This article is protected by copyright. All rights reserved.